8. END-CAP YOKE

This chapter describes the analysis and construction of the endcap yoke. The overall configuration of the endcap region is shown in Fig. 8.1. This chapter is concerned with the yoke portions of the endcap, namely YE1, YE2, YE3 and YN. These elements form the magnetic portion of the endcap.

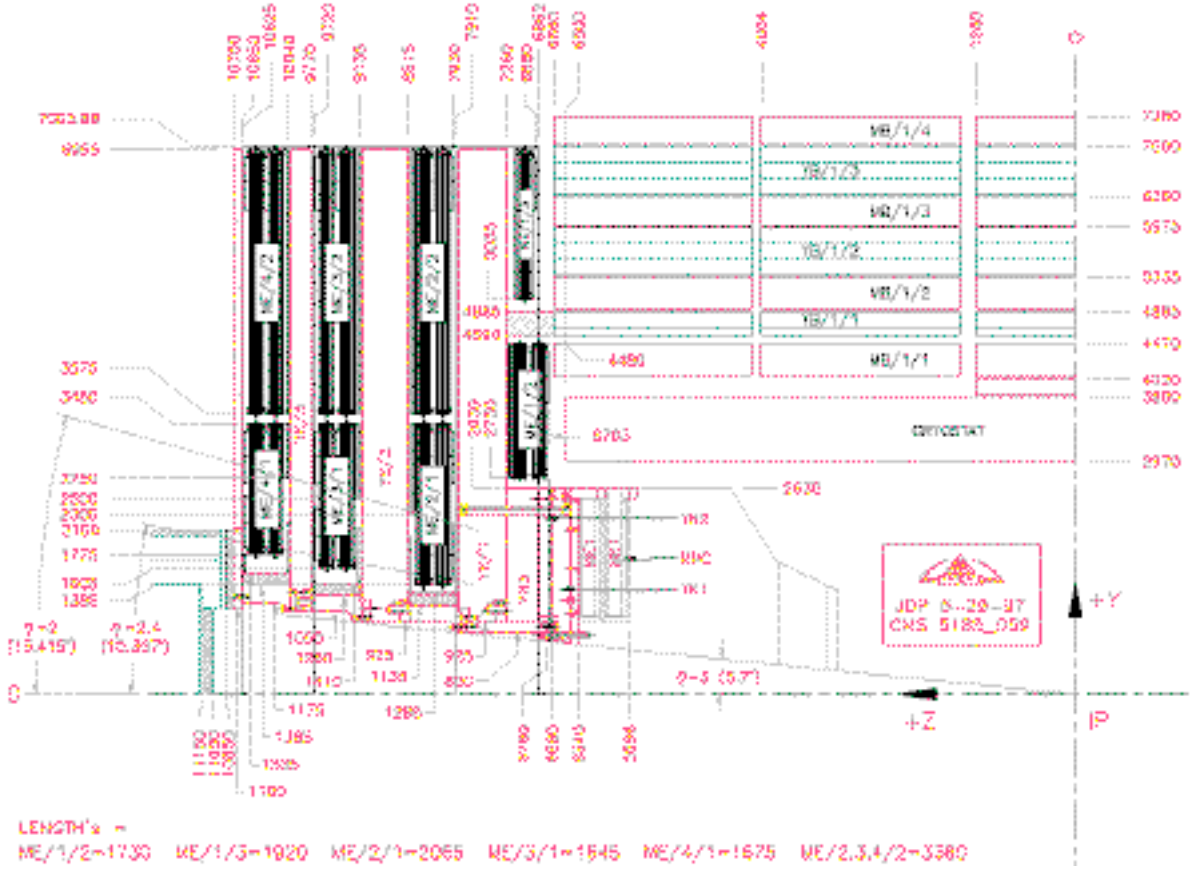

Fig. 8.1: Longitudinal view of endcap region.

8.1 STRUCTURAL ANALYSIS

An analysis has been performed on the steel structure of the endcap using the ANSYS® general purpose finite element program. The analysis is for a full 3-dimensional model of the endcap. In this model each disk is fabricated from 24 sectors. The effects of gravity and magnetic loads have been modelled.

A three dimensional analysis is required because the construction of the disks from many sectors can only be represented in a 3-D model. Also effects of gravity on a mostly round object are best analysed with a 3-D model. In this model, the endcap calorimeter and all attached objects are assumed to be 300 tonnes total. The calorimeter is assumed to have a bulk stiffness value equal to steel.

8.1.1 Purpose

The two primary areas of concern that have been addressed with this analysis are:

1. The stresses on the connections between disk segments when the disk is loaded

magnetically. The magnitude of the total magnetic load on YE1 is roughly 10 times larger than the gravitational load. This load is reacted against the ends of the barrel iron. The magnetic forces are not applied evenly over the surface of the disk but, instead, are concentrated toward the centre of the disk. The result is that the region of the disk inside, radially, of the barrel support is pulled towards the interaction point while the region outside is pivoted away (Fig. 8.26, p. XX). This deflection generates tensile forces in the segment connectors on the face closer to the IP and compressive forces in the connectors on the opposite face.

2. The stresses and deflections in the carts supporting the three disks. This investigation can focus on an examination of the cart for YE1 since the configuration of this disk is the hardest to accommodate. The nose assembly on YE1 is a large overhanging load which not only increases the total weight on the cart but also produces a large moment on the connection between YE1 and the cart. The requirements of the carts for YE2 and YE3 will be much less stringent.

8.1.2 The Model

The model assumes a disk constructed from 24 sectors. We have also analysed a disk made from one piece. The maximum deflection for a solid disk is about 7 mm under magnetic loads. This represents the lower boundary of the deflection.

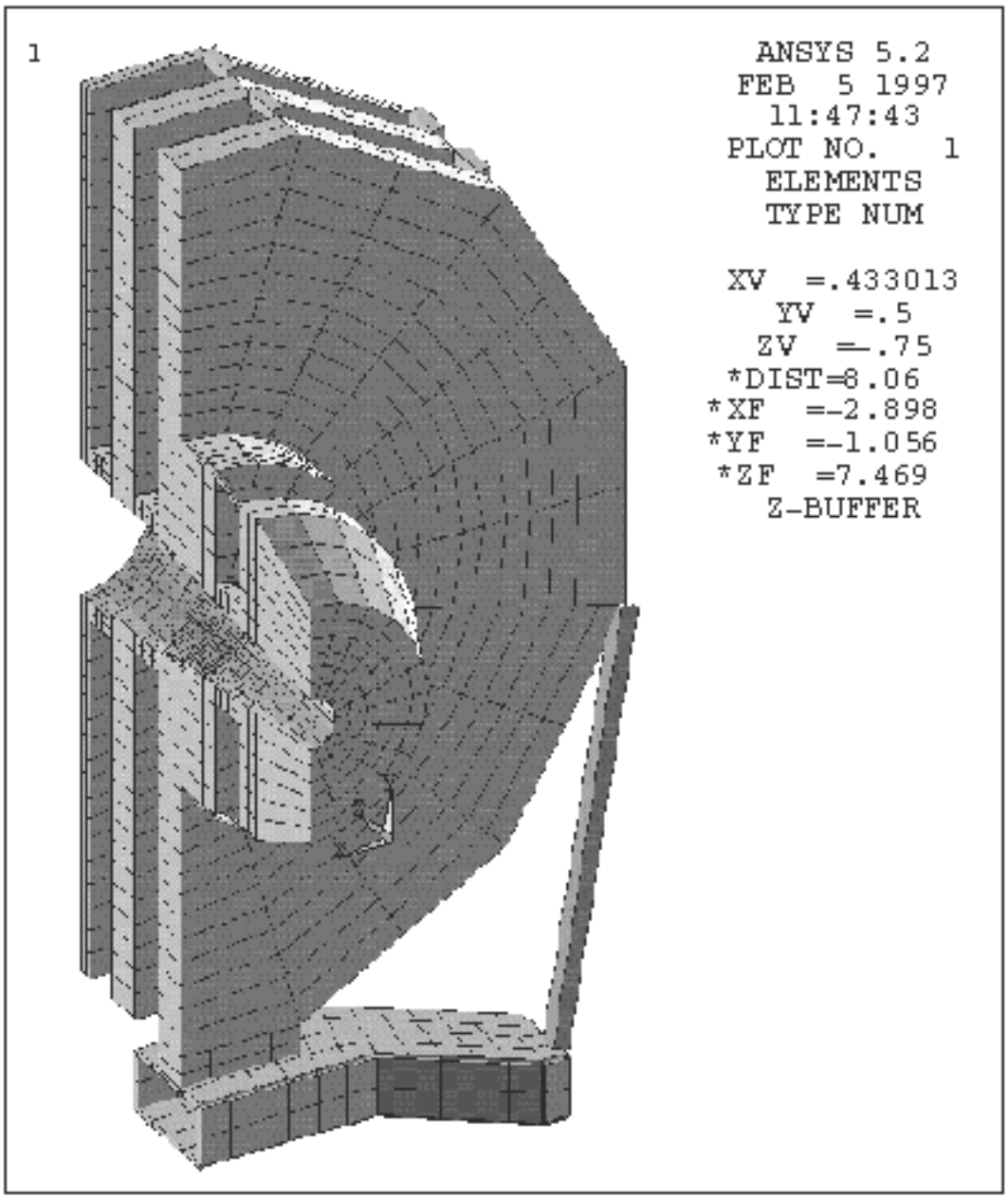

Fig. 8.2: Finite element model of endcap.

Figure 8.2 shows the 3-D finite element model of YE1 with its cart and the overhanging nose assembly. As shown, only half of the disk is modelled with a symmetry boundary condition on the cut plane replacing the missing half. The nose has been sized to match the weight and centre of mass location of the current design. Figure 8.2 also shows the model of the rest of the endcap with the carts for YE2 and YE3 replaced by simple position constraints. The support of each of the three disks is independent enough that the carts for YE2 and YE3 can be examined independently.

The two versions of the model that are of interest are:
1. YE1 and its cart with gravitational loading and the 300 tonnes cantilever load.
2. All three disks with gravitational and magnetic loads.

The disks are made from 8-node brick elements with 3 degrees of freedom at each node. The cart is made from 4-node shell elements (6 degrees of freedom at each node) since it is

anticipated that the raw material will be steel plate. The support pad between the cart and the disk is made from 8-node brick elements that have 6 degree of freedom of at each node.

All nodes that would be connected to the unmodelled half, if it were present, are given a position constraint against deflection in the x direction but allowed to move in the y and z direction. This is the above-mentioned symmetry condition that allows the modelling of only half the structure. There are position constraints against vertical motion applied to the footpads of the cart. When the entire endcap is modelled, with magnetic loads included, position constraints against motion in the z direction are applied to YE1 at the same radius at which the barrel would constrain the disk. If YE1 is modelled alone, without magnetic loads, then a single node on one of the footpads is constrained in the z direction to prevent rigid body motion in that direction.

The 1.23% slope of the floor in the hall is accounted for by applying a vertical gravitational acceleration of 9.809 m/s^2 and a horizontal gravitational acceleration of 0.121 m/s^2. In all models the horizontal component acts in the minus z direction, the direction that adds to the moment in the cart already present from the overhanging nose.

The disks are separated by the shield rings. These rings are attached to one disk and touch the next disk. To model the shield ring between YE2 and YE3, the two coincident circles of nodes at the inner radius of the contact area between YE3 and this shield are coupled so that they have the same z displacement but are not coupled in any other way. This is based on the assumption that this region will be in compression (an assumption that is shown to be correct by inspecting the forces later). This does neglect any sliding friction between the shield and the disk.

At the other end of this shield the outer ring of nodes is anchored firmly (with constraint equations) to the face of YE2. This means that the outer ring of nodes at this end of the shield maintain their position with respect to the adjacent nodes on the surface of YE3. This shield is, therefore, fixed with respect to YE2 and slides on the surface of YE3. The same arrangement is repeated with the shield between YE2 and YE1. This ensures that the weight of each disk rests predictably on its own cart and is a reasonable model of what would actually be designed.

The construction of the disk from pie-shaped segments is imitated by the way the segments of the model are joined. On the surface of the disk farther from the IP all nodes in each sector are merged with the corresponding nodes in adjacent sectors. Since these joints connecting the sectors will be in compression this is the most realistic connection. On the opposite surface, closer to the IP, nodes are merged at the outside edge, the inside edge and four other fairly equally spaced points between. This models the case where six connectors, or ties, are used along each seam on this face (see Table 8.1). The nodes in the middle plane of the disk between the two faces are not joined as this would give an unrealistically rigid connection.

Table 8.1
Connections between sectors.

No.	Radius	Location
1	0.8 m	Inside radius of disk
2	2.013 m	An intermediate point
3	3.227 m	An intermediate point
4	4.74 m	Radius of YB1, Z support for magnetic loading
5	5.709 m	An intermediate point
6	6.955 m	Outside radius of disk

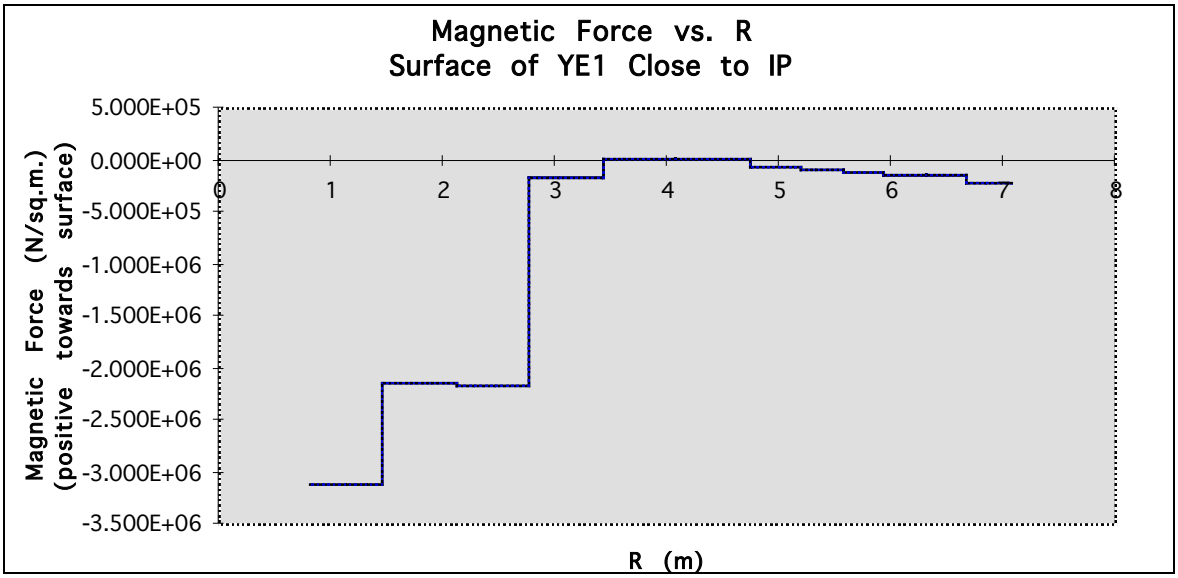

Fig. 8.3: Axial force distribution on YE1 at Z = 7.26 m.

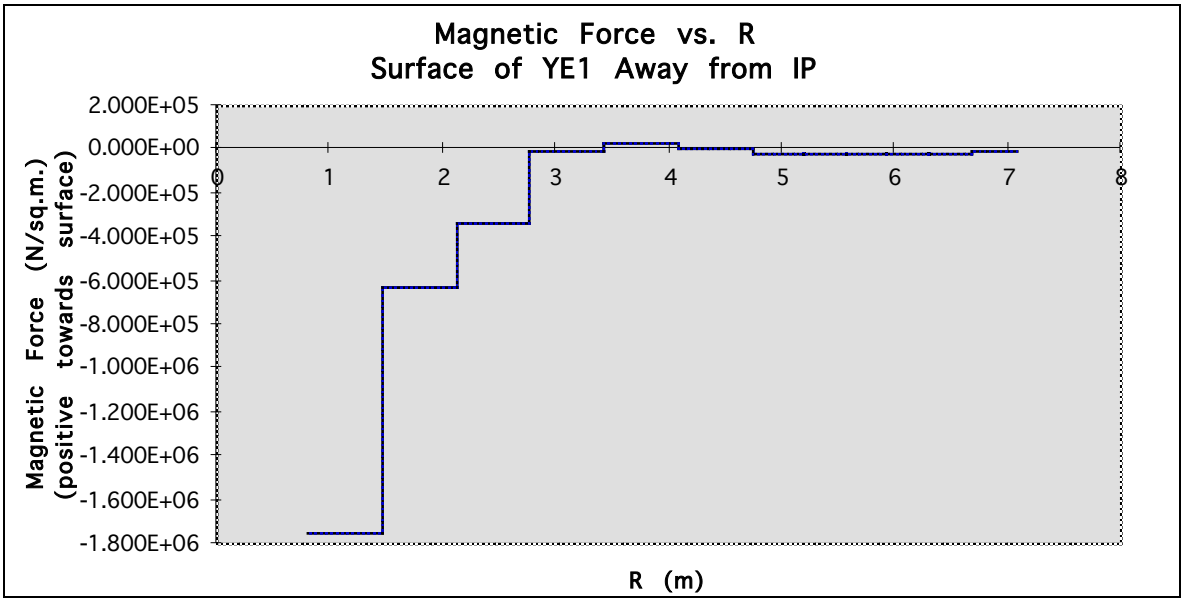

Fig. 8.4: Axial force distribution on YE1 at Z = 7.86 m.

The loading is derived from a 2-D, axisymmetric, magnetic analysis, also done in ANSYS, that predicts loads in the r and z direction at a number of nodes on the surface of each big disk and on the two steel disks of the nose [8-1]. On YE1 and YE2 the z forces are roughly an order of magnitude larger than the r direction forces. On disk YE3 the forces are comparable magnitude but the forces on YE3 in general are much less than on YE1 and YE2. Since, in addition, the radial forces will be less likely to distort the disks than those in the z direction, the radial components have been ignored.

The forces on each face of the 3 large disks were divided radially into 12 groups corresponding to radial rings of elements. The force in each area divided by the area of the ring yields the pressure which is applied to the elements in that area. Plots of these pressures are shown in Fig. 8.3 and Fig. 8.4 for disk YE1 at z = 7.26 and z = 7.86 respectively.

8.1.3 Model Results

Magnetic and Gravity Loading

The predicted deflection of the endcap under magnetic and gravity loading is shown in Fig. 8.26, p. XX. The nose on YE1 is pulled towards the IP about 14 mm. The outside edge of the disk is levered in the opposite direction about 8 mm. Due to the connections between the disks, YE2 and YE3 have equal deflections. This shows that the entire endcap calorimeter is predicted to move toward the IP by about 14 mm as a rigid body. Since the endcap calorimeter is made from non-magnetic materials, no additional distortions are expected in the Z-direction. Therefore, the space allocation for the endcap calorimeter must include at least 14 mm in the Z-direction as the magnetic field is energised.

Figure 8.27, p. XX, shows the deflection of the endcap in the Y-direction (vertical) due to magnetic and gravity loading. It shows that the endcap calorimeter deflects down by about 2 mm. This is almost entirely due to the gravity load on the connections of the endcap calorimeter to YE1. The endcap calorimeter is assumed to be 300 tonnes total and to have a bulk stiffness value equal to steel. This, of course, is a simplifying assumption made for the purposes of this model only. This is valid here because we are only interested in the effects of the cantilever load on the endcap. However, the structure of the endcap calorimeter is much different. It is made from copper plates with space for scintillators. It will not have a stiffness value equal to steel. Therefore, the 2 mm sag is only due to the support. The sag within the endcap calorimeter must also be added to this number. The space allocation for the endcap calorimeter must include both numbers.

Gravity Loading of YE1

The predicted Z deflection of YE1 and its cart, under gravity loading only, is shown in Fig. 8.28, p. XX. Under this condition the support is only on the cart, i.e. the detector is open and the endcap is not supported on the barrel. This figure shows a Z distortion for the endcap calorimeter of about 1 mm toward IP at the top and 2 mm away from IP at the bottom. This is due to gravity loading of the cantilevered endcap calorimeter which causes a bend in middle of the YE1. In this figure the brace is represented as a line.

The predicted Y deflection of YE1 and its cart, under gravity loading only, is shown in Fig. 8.29, p. XX. The total deflection is about 4 mm in the -Y direction. It is, again, due to gravity loading of the cantilevered endcap calorimeter. The sag of the endcap calorimeter itself, must again be added to this number as explained above.

These figures show that YE1 is not vertical by about 5 mm and the endcap calorimeter

is displaced by about 6.5 mm (vector sum of 4 mm Y and 5 mm Z deflections). To close the detector, the endcap must be made closer to vertical by lifting the front supports. This operation will make YE1 vertical on the average. However, due to its bend, it will not be vertical everywhere. As the detector closes, it is likely that the endcap will touch the supports on some but not all points. Then, when the field is turned on, then YE1 will basically "flatten" against the barrel. This is not desirable. A better approach is to make the supports with different lengths so the endcap touches all supports prior to turning on the field. This will avoid large motions. It may also be desirable to preload the supports.

Sector Connections

Figure 8.5 shows the forces on a sector schematically. The tangential forces between two sectors at Y = 0 for both sides of the disk are plotted in Fig. 8.6 and Fig. 8.7 for combined loading and for gravity only loading respectively. For combined loading, they are greatest at the second tie out from the inside, at a radius of about 2.01 m. The load in this tie is about 4.5 MN. The inner tie is carrying a load of about 3.2 MN. For gravity loading only, the directions switch and the forces are smaller. Therefore, the magnetic load is the main load on the ties between the sectors.

Tie Rod Forces

The nose is connected to YE1 with 24 tie rods near its outer radius. The tie rods are modelled as 80 mm diameter cylinders. These tie rods are under tension. The total tension on all tie rods is 52.4 MN. The maximum tie rod tension is 2.62 MN at the top and 1.89 MN near the bottom. The average tie rod tension is 2.18 MN. The non-uniformity is due to the moment generated by the cantilevered calorimeter.

Z Support Forces

The Z supports are spacers between the endcap and the barrel, i.e. between YE1 and YB/2/1. They occupy the radial space between the muon chambers ME/1/2 and ME/1/3. There will be 24 Z supports arranged in pairs every 30°.

The total Z support force is roughly 85 MN. This is the total magnetic load on one endcap. This force is all transmitted through the barrel rings and reacted by the equal and opposite load on the other endcap.

The Z support forces on the 24 Z supports are not equal. They vary slightly in value at different azimuths. This is due to asymmetry introduced by the cantilever load. The maximum Z support force is 3.7 MN and the minimum Z support force is 2.8 MN.

Endcap Calorimeter Connection

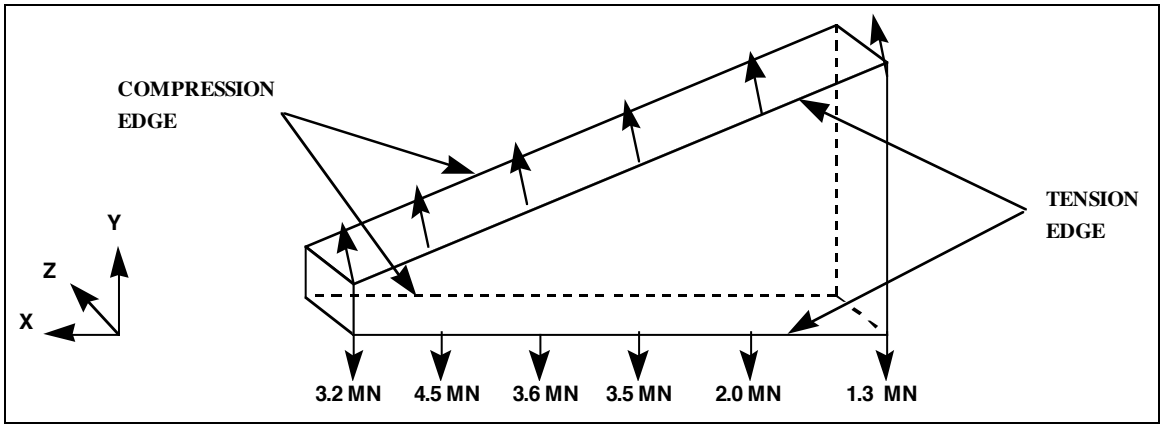

Fig. 8.5: Loads on a single sector.

The endcap calorimeter attachment to the nose is modelled with 12 tie rods near the outer radius of the nose. The tie rods are modelled as a 64 mm diameter cylinders. These tie rods are under tension. The total tension on all tie rods is 25.6 MN. The maximum tie rod tension is 4.66 MN at the top and 1.05 MN near the bottom. The average tie rod tension is 2.13 MN. The non-uniformity is due to gravity and due to the 4 struts spanning the ME1 space. (These struts are 90° apart).

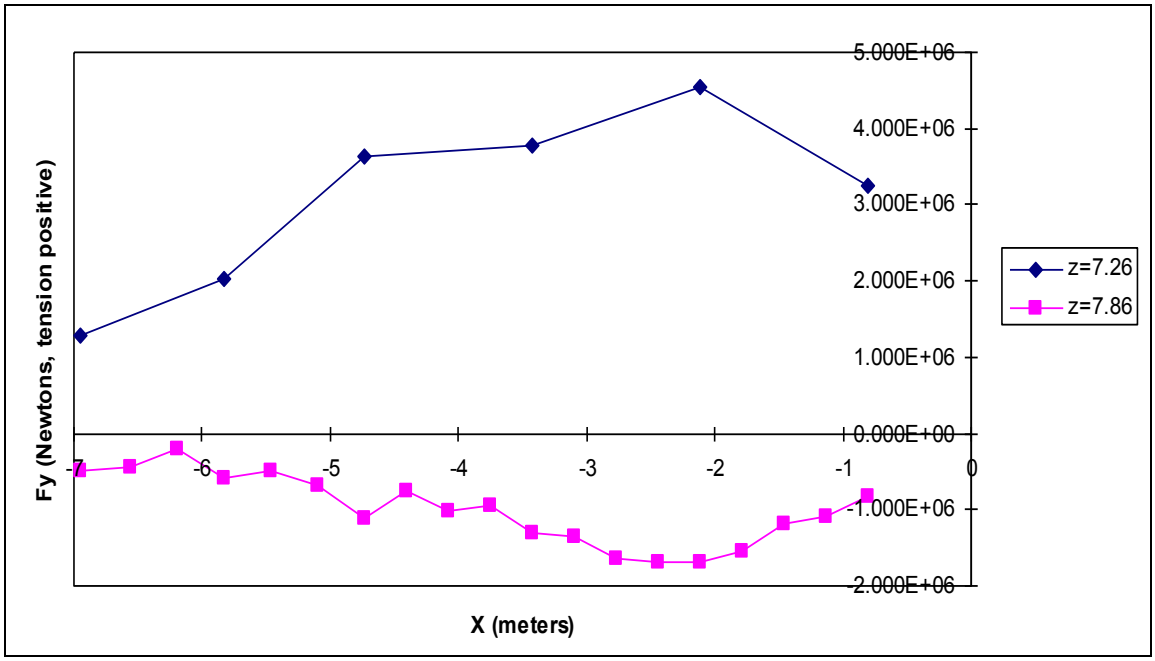

Fig. 8.6: Tangential forces at Y = 0 for gravity and magnetic loading.

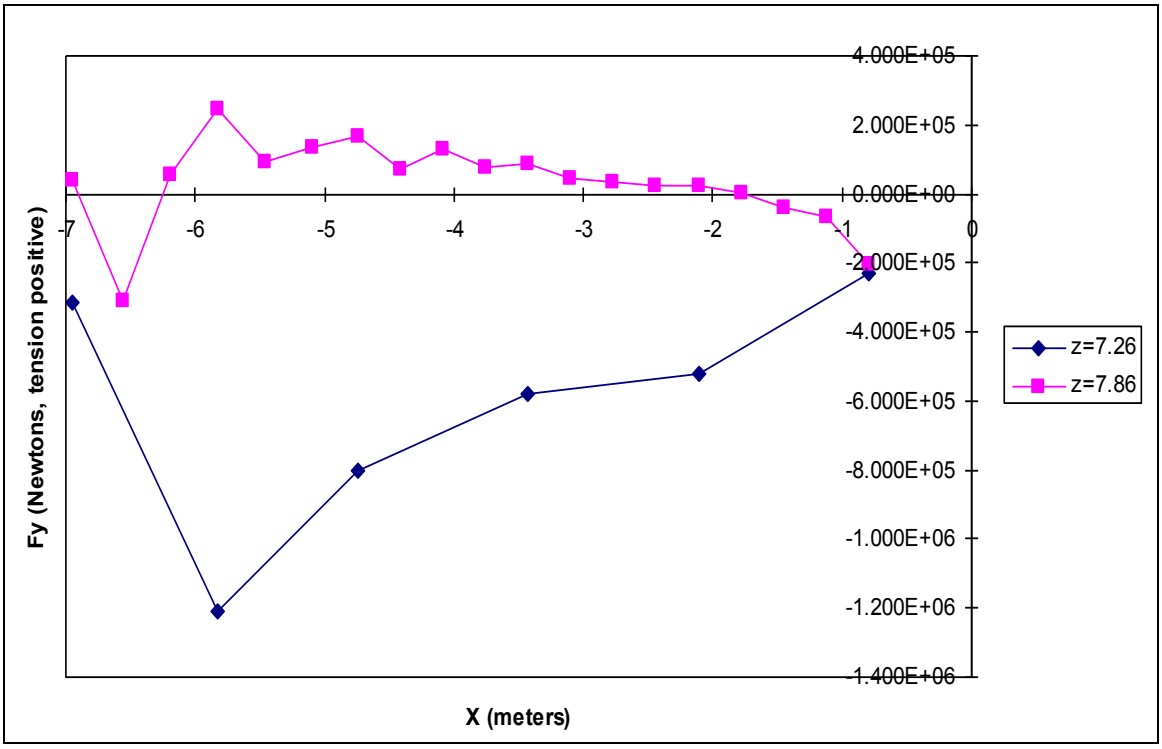

Fig. 8.7: Tangential forces at Y = 0 for gravity loading only.

8.2 ENDCAP YOKE CONSTRUCTION

8.2.1 Design Criteria

The criteria for the mechanical design of the endcap absorber are as follow:

1. Uniform steel composition and symmetrical construction to ensure proper return for magnetic flux.
2. Safety during detector operation under severe magnetic loads.
3. Safe support for endcap calorimeter and other equipment attached to the endcap. Total supported mass is about 300 tonnes for each endcap.
4. Safe support of the disks under gravity loads. Total self mass is 3800 tonnes.
5. Safe operation during access to the endcap and to interior of the detector.
6. Design that can be produced by existing technology at several steel mills and large machine shops. This is important because the requirements for the size of the endcap limit its production to a very few facilities.
7. Support of endcap muon detectors in a very rigid and stable manner.
8. On-site assembly to be compatible with conventional facilities, and with schedule.
9. Cost to be within projections.

In order to satisfy points 2-4, safe stress levels have to be chosen. As a guide we have used the American Institute of Steel Construction (AISC) Manual for Steel Construction [8-2]. This code is a thick book. It is not directly applicable to the design of large magnets of very thick section. It is mostly applicable to conventional steel construction. However, we intend to satisfy the intent of this code. We have reviewed the code and believe the following criteria to be applicable:

- Maximum stress in tension only members to be less than 60% of yield strength on gross section, and 50% of ultimate strength on net area.

- Maximum combined stress (Von Mises) in all other members to be less than 66% of yield strength.

Other design criteria are addressed in the following sections.

8.2.2 Endcap Yoke Components

The endcap yoke consists of many distinct items. Table 8.2 lists the items along with their quantity, mass and reference drawing number. It must be noted that some items, such as each of the three disks, are assemblies of many other items. For brevity, these sub-components are not listed. The drawings are on file but have not been included in this report. The CMS + and - sides are ignored for the purposes of this list, i.e. the two endcaps are assumed to be identical. The total mass for both endcap yokes is 4600 tonnes.

8.2.3 Overall Disk Tolerances

The overall disk needs to meet certain tolerances of size and form in order to satisfactorily interface with other components.

Figure 8.8 shows a schematic of a thick disk with overall tolerances.

The tolerances of form and position define the overall boundary of the disk. Several things should be noted:

1. The disk thickness varies between 590 mm and 600 mm.
2. The boundary of the centre hole is within 1 mm of its true form.
3. The 12-sided boundary of the disk is within 5 mm of its true form.
4. The entire disk is contained in a volume bounded by:
   - A 12-sided shape that is 13922 mm across,
   - by a cylinder that is 1796 in diameter and is centred on this shape,
   - and by two planes that are 600 mm apart.

Table 8.2
Endcap Yoke Top Level Parts list.

Item	Ref. Drawing	Qty (each)	Unit Mass (tonne)
YN1	5185D074	2	38
YN2	5185D062	2	23
YN3	5185D063	2	62
Inner YN1-YN2 Connection Ring	5185C064	2	2.3
Inner YE1-YN3 Sleeve	5185C066	2	5.3
YE1 IP Side ID Ring	5185C065	2	1.8
YE1 Disk Assembly	5185E123	2	721
YE1 Outside ID Ring	5185C067	2	1.9
Main Nose Tie Rod	5185E034	40	0.1
YE1 Cart Assembly		2	90
YE1-YE2 ID Spacer Ring	5185C068	2	8.5

YE2 IP Side ID Ring	5185C065	2	1.8
YE2 Disk Assembly	5185E122	2	721
YE1 Outside ID Ring	5185C069	2	2.1
YE2 Cart Assembly		2	90
YE2-YE3 ID Spacer Ring	5185C070	2	10.2
YE3 IP Side ID Ring	5185C071	2	1.5
YE3 Disk Assembly		2	299
YE3 Outside ID Ring	5185C072	2	1.4
YE2 Cart Assembly		2	90
YE2-Outside ID Spacer Ring	5185C073	2	12.1
ME/4 Shield Small Ring	5185C119	2	7.9
ME/4 Shield Large Ring	5185C120	2	108

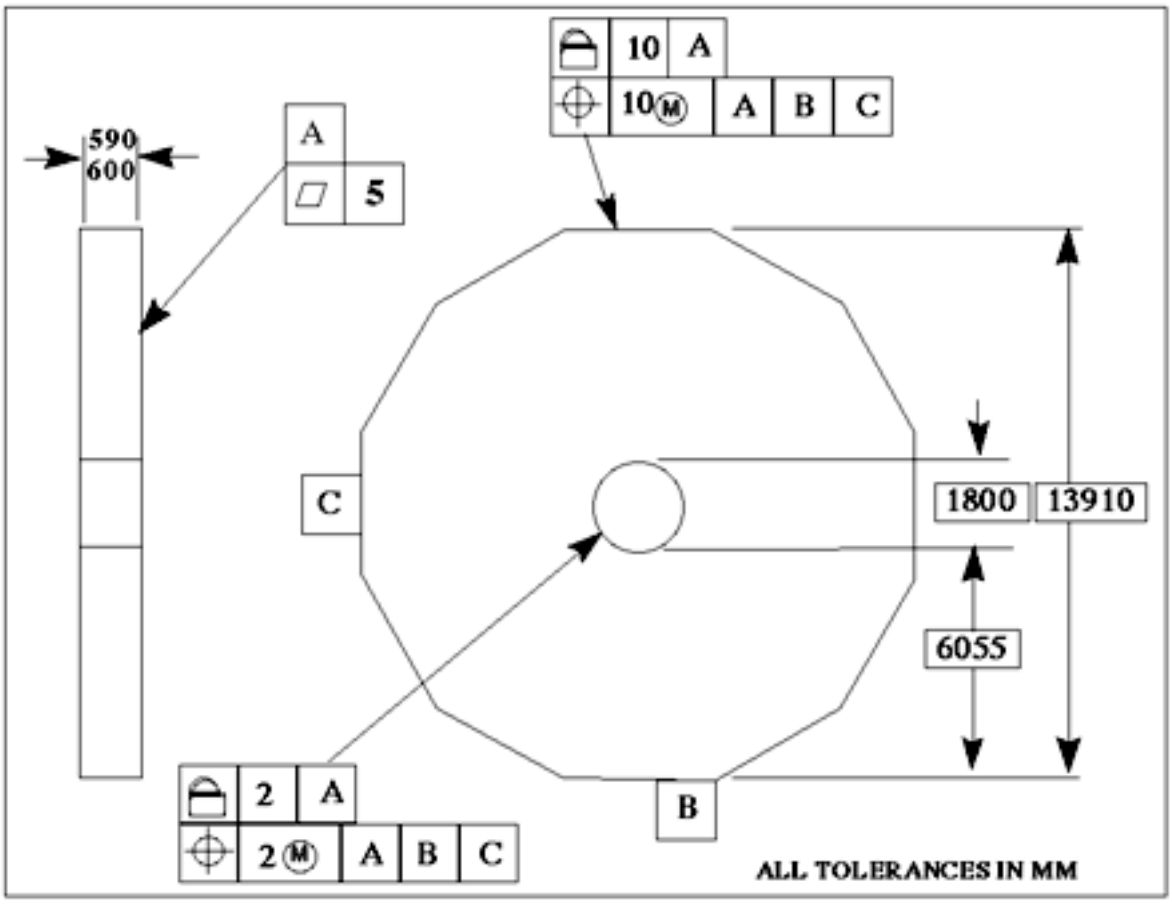

Fig. 8.8: Overall disk tolerances.

8.2.4 Design Options

Several designs have been investigated. The main criterion is that any design has to be within the capabilities of standard steel mill and large machine shop technology. The options fall into two sub-categories:

1. Mechanically joined options. Blocks are pinned and bolted, or similarly joined, to form a disk.
2. Welded options. Rectangular blocks are welded together by Electroslag (or similar) welding process to form a monolithic disk, (see Chapt. 10).

Welded options require on-site assembly as the fully welded disk is too large for transportation. Mechanically joined options can be preassembled at the factory, disassembled and then reassembled at the site. There are cost, schedule, and performance trade-off issues with either option.

Presented below is a reference design using the mechanically joined option. It is given as a reference design because many variations are possible for this option. It is our intention to present this reference design as a possible option to vendors in a request for tender. The vendor can either offer a proposal for construction based on this design, or chose a variation of it. We intend to leave options open for vendors to propose better and/or cheaper options. However, we believe it is important to have a reference design that is well analysed and has a very good chance of meeting cost and performance criteria.

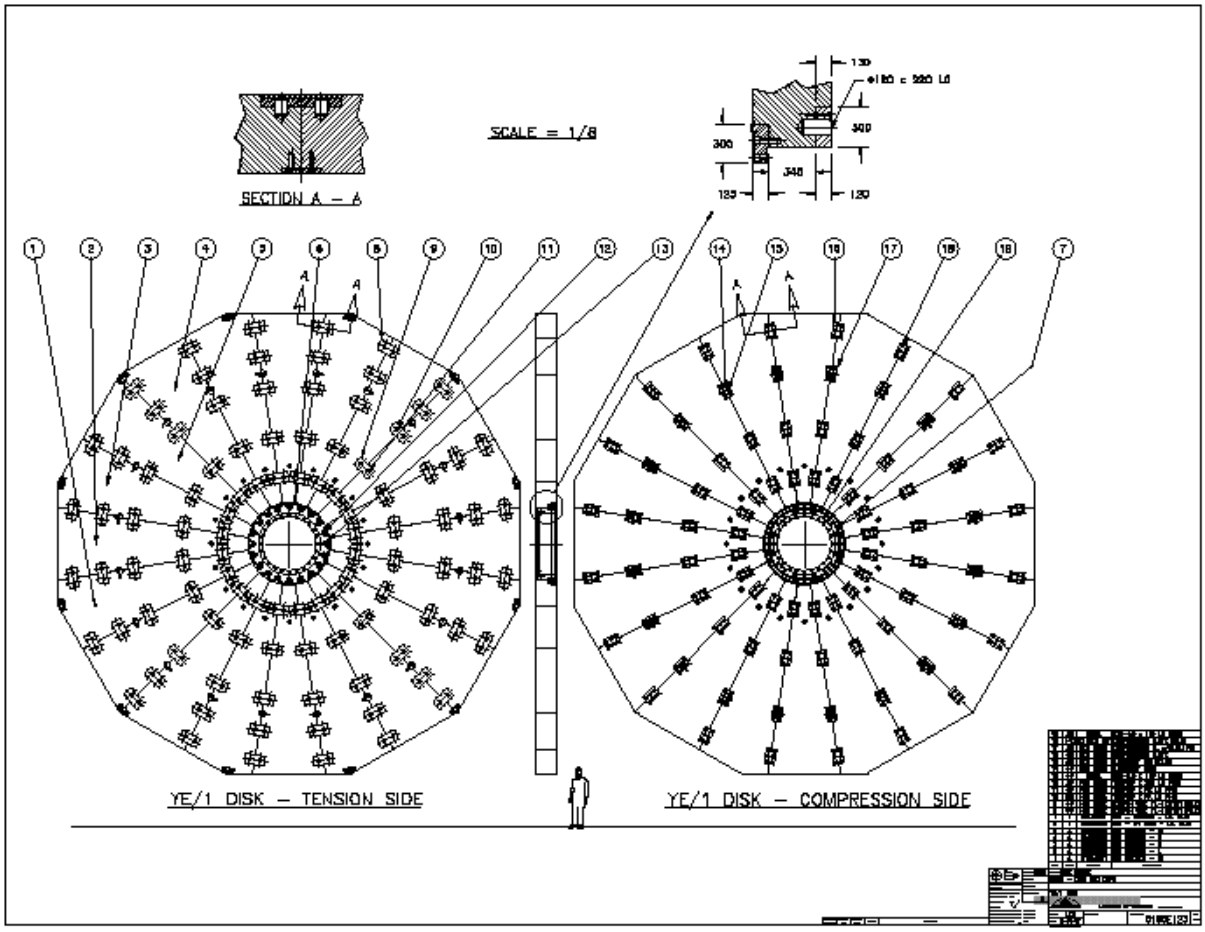

Fig. 8.9: Typical disk construction from 20 sectors.

8.2.5 Mechanically Joined Option

Figure 8.9 shows a typical disk subdivided into 20 sectors, joined by pins and fasteners. These sectors can be cut in pairs from plates of steel as shown in Fig. 8.10. The number of sectors can be more or fewer. Fewer sections are preferred as they reduce the number of joints. However, fewer sections require larger plate sizes which may not be available. From our study of steel mill capacity so far, we believe that a 20-sector construction is a possible compromise.

Figure 8.9 also shows a typical sector connection. Section A-A. On the compression side of the disk, away from IP, strap plates with bolts are used. On the tension side, toward IP, a plate and two pins are used. At the centre of the disk, a ring is fitted to the sectors. It is important to note that the pinned connections must be designed in a way that can be verified for proper fit and tolerance at the factory. However final assembly of the joints will occur once at the site.

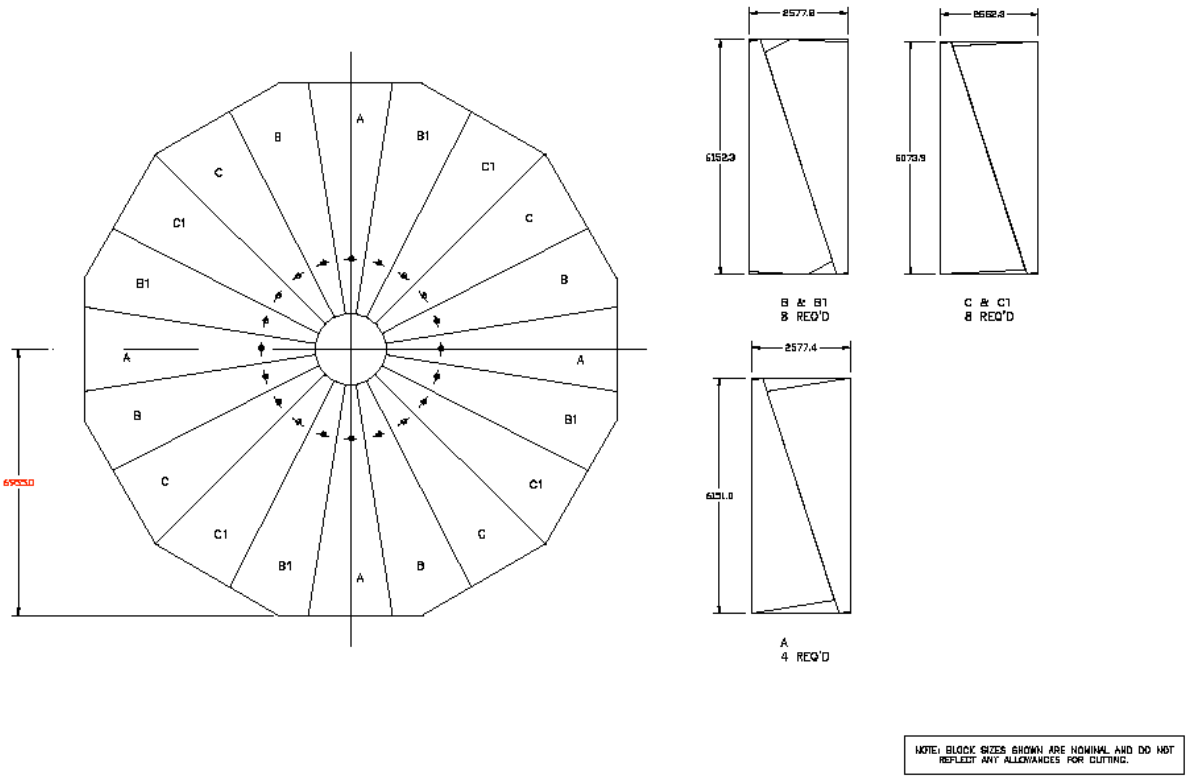

Fig. 8.10: Cutting of plates for a 20-sector construction. Note that the plate sizes are nominal and do not reflect any cutting allowance.

Figure 8.11 shows a typical machined block without tolerance. This drawing does not have any tolerances as of yet. However, it is expected that most critical dimensions will need control to about 0.5 mm. Detail A shows the features for the connection on the compression side. Detail C shows the detail for connections on the tension side. Detail B shows features for alignment pins for assembly of the sectors into the disk.

It is anticipated that to achieve proper fit between these large blocks, mating features between two blocks will have to be machined together. This can be done by stacking pairs of mating blocks and machining these features jointly.

Figure 8.12 shows the erection sequence for a typical disk. This drawing shows the use of a starting block which is attached to the support cart. This variation is most applicable for YE2, where the support cart only spans the bottom two to four sectors. The starter block may in fact be part of the cart structure.

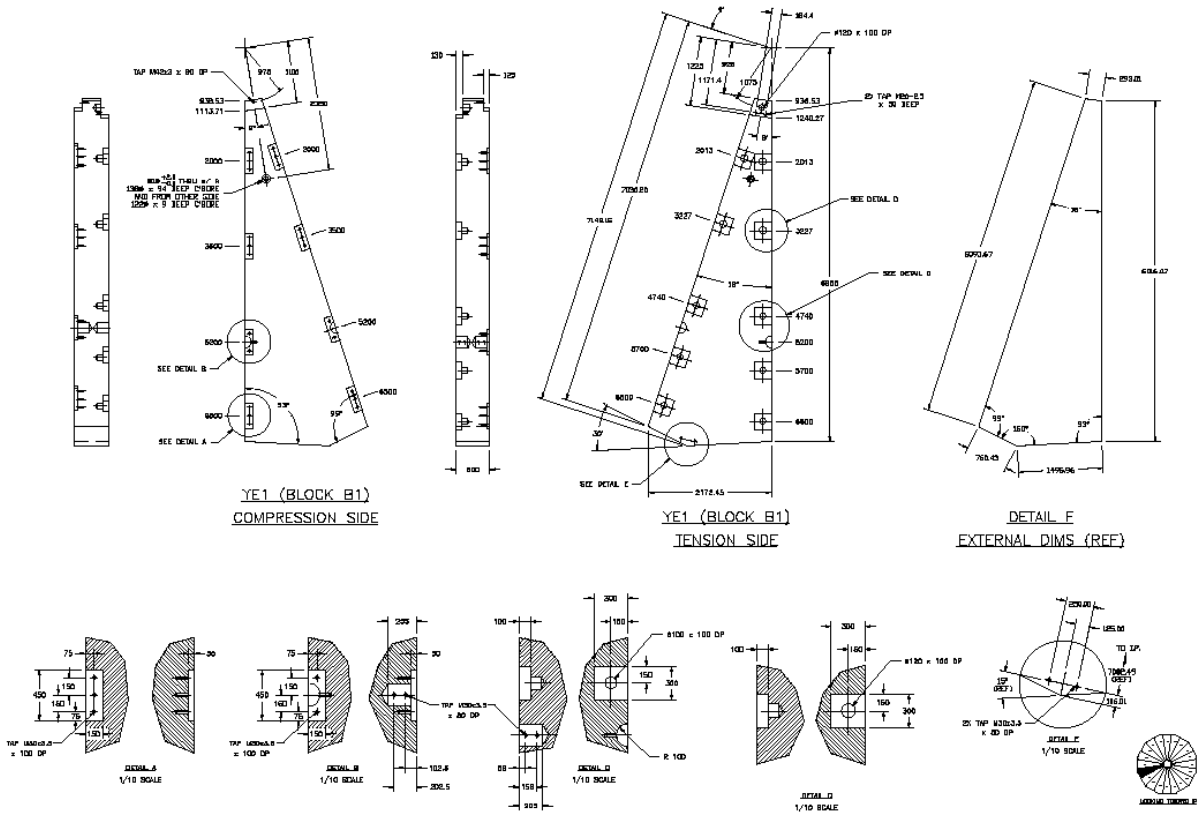

Fig. 8.11: Typical machining of a sector block showing connection features per our reference design. All dimensions are basic, no tolerances applied.

Individual block tolerances and gravity will require careful analysis of errors in this scheme. It is anticipated that the last block will have to be machined to fit. This is done by measuring the space left for the last block with respect to reference points on adjacent blocks and then determining the final shape of the last block.

8.2.6 Joint Alternatives

As mentioned earlier, there are many possible variations for a mechanical joint. The criteria for a joint are as follows:

- Ease of assembly and possible disassembly. This will allow for possible correction to a block.
- Verification prior to final assembly at site. This will allow full erection of disk at the factory and will help minimise assembly time on site.
- Deterministic design of load carrying parts. The joint can be analysed in detail to determine its proper operation under all loading conditions.
- Possibility of introducing joint preload. This will allow for smaller overall distortions and will help with life expectancy of the joint.

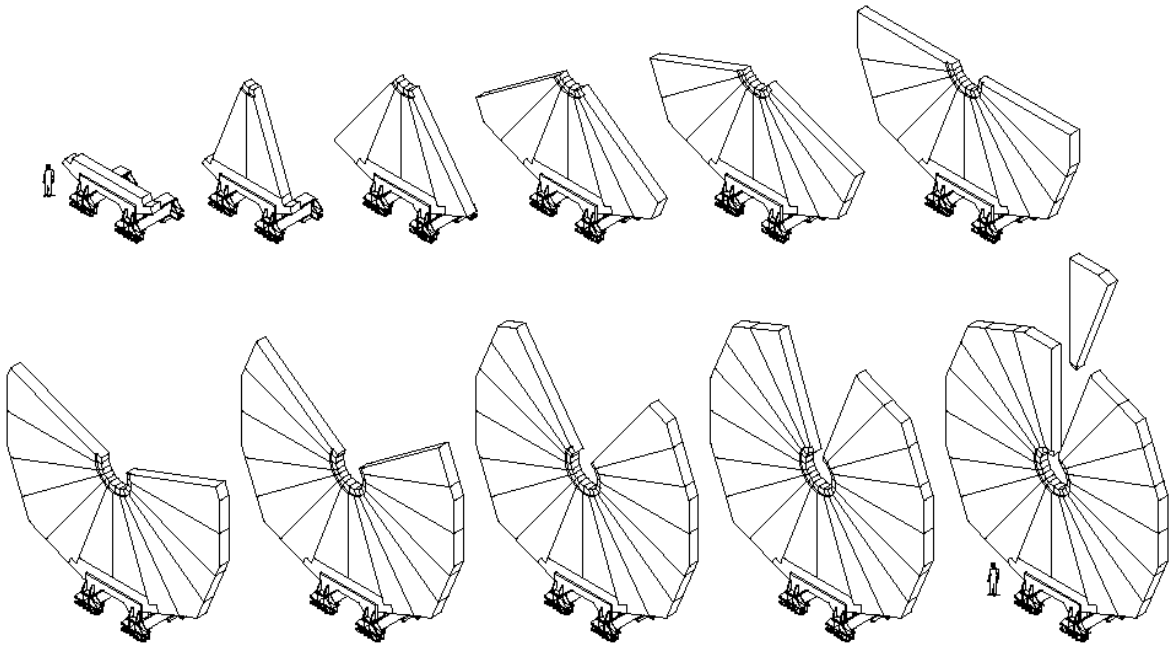

Fig. 8.12: Erection sequence. Last block machined to fit.

Many designs can satisfy these requirements. Presented below is one alternative. It must be noted that any design must minimise the amount of machining of the blocks. It must also minimise voids as they degrade magnetic performance of the disk at these locations by causing field non-uniformity. It is anticipated that this will not be a major concern unless the joint design has very large voids. The sensitivity of the magnetic performance to voids has not been studied in detail.

8.2.7 Joint Preload

In 8.1.2, a disk is modelled with 24 sectors. Each sector is attached to adjacent ones by letting them share a single common point (node) at several joint locations. In this case, regardless of the distortion field, this node remains common, i.e. the sectors are always attached at this point with zero separation. The interpretation of this is that the joint is assumed to be preloaded to a level where it never separates. If no preload is present, a small separation will occur at the joint and the overall distortion of the disk is likely to be slightly higher. This has not been modelled or calculated as of yet. It is anticipated to have a small effect on overall distortion. However, joint preload may be essential due to other factors such as aiding in assembly, and for longer life in cyclic loading.

For a large joint, application of a preload may require innovative approaches. One approach would be to use the thermal expansion of parts to introduce a preload. In the joint design shown in Fig. 8.16, no preload is assumed.

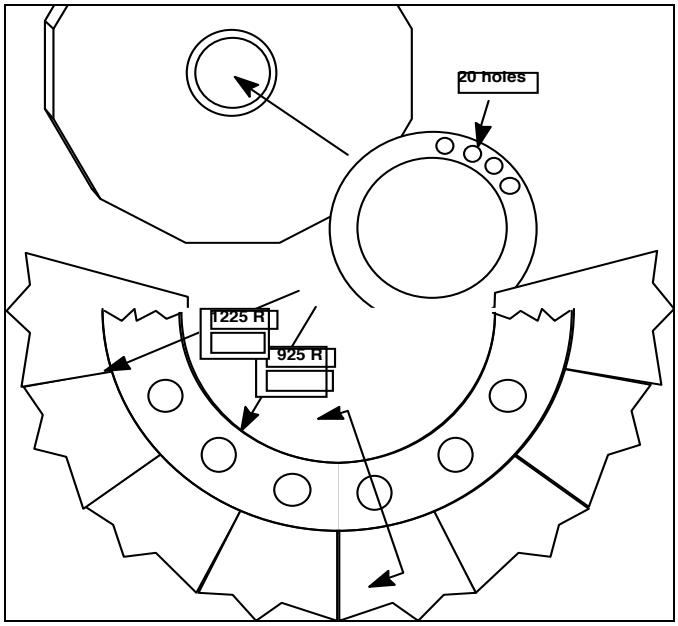

Fig. 8.13: Central ring of YE1 disk (YE2 and YE3 have similar rings).

8.2.8 Center Ring Connection

The joint at the centre of the disk is under high loads also. A central ring will be required to tie the tips of the blocks together. A ring is chosen, instead of individual plates, because the pins get very close to each other. A centre ring will also aid in the assembly process by providing a reference circle in the centre of the disk.

Figure 8.13 shows the centre ring that is fitted into the centre to resist this load.

Figure 8.15 shows the connection of the ring to the disk.

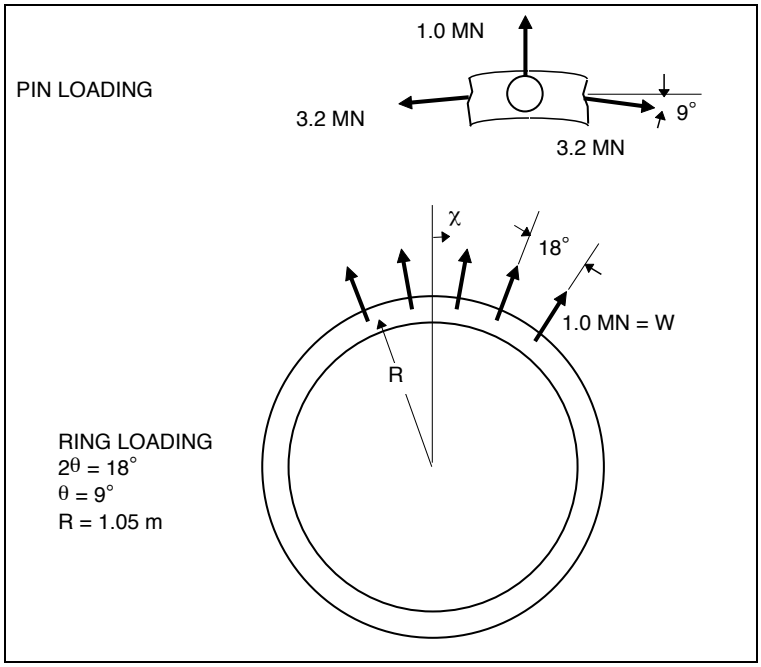

Fig. 8.14: Loading of central ring and pins.

8.2.9 Center Ring Loading

As the disk deflects toward the IP, each individual sector exerts a radial force on this ring through the pins. This load causes a combined tension and bending load on the ring cross section and a combined bending and shear on the pins.

In figure 8.5, the loads on a single sector are shown. The innermost force of 3.2 MN is resisted by the ring. This force is in a tangential direction, however, the resultant force on the ring from the pin will be in a radial direction.

In figure 8.14, the loading condition of the pin and the central ring are shown. Note that the analysis was done for a 24-sector construction. However, the plan is to build the disks from 20 sectors, so this force is applied at 20 locations on the ring. The analysis will be updated to reflect the actual number of sectors as the design progresses.

8.2.10 Center Ring Stress Analysis

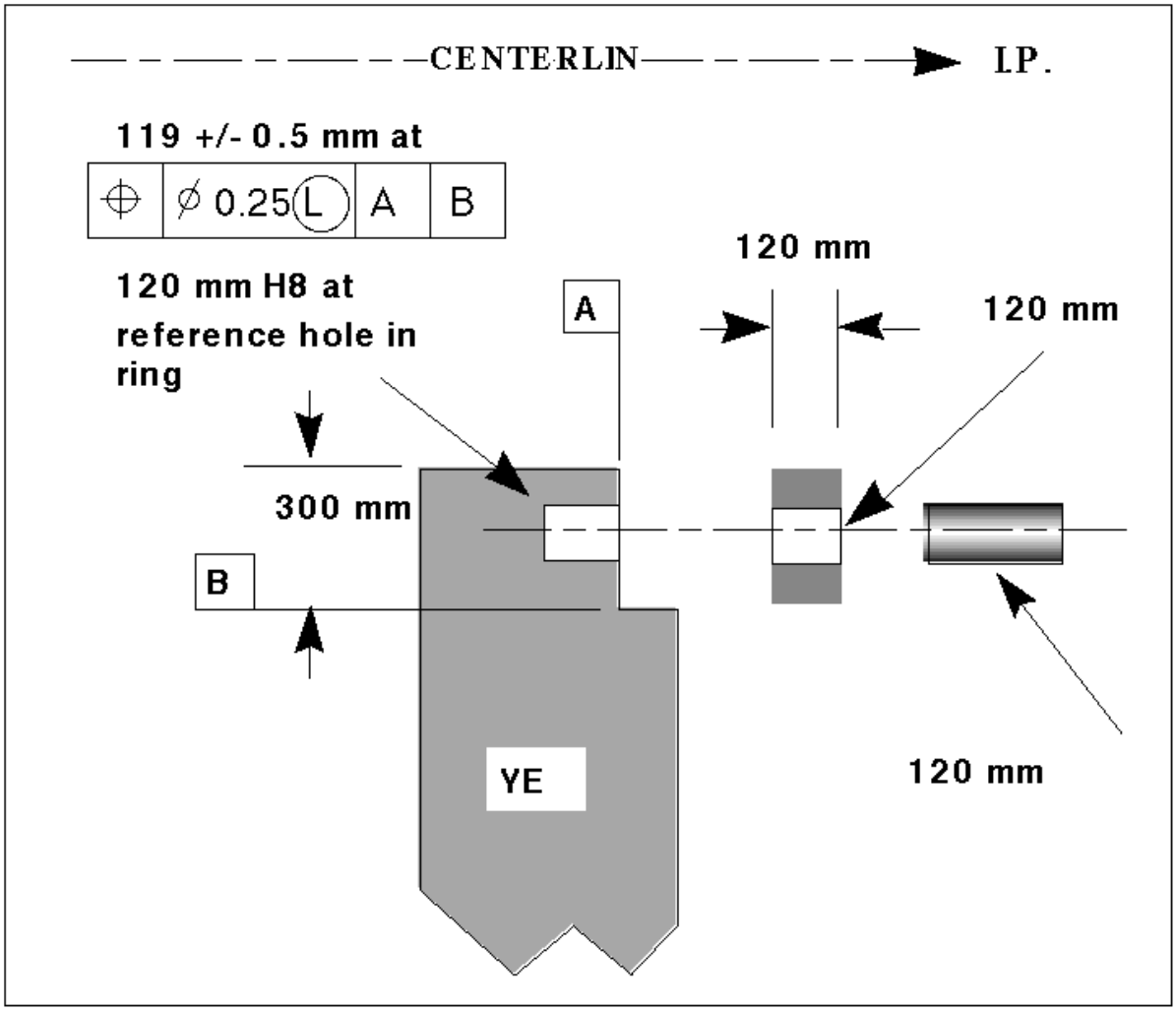

Fig. 8.15: Connection of central ring to YE.

The centre ring is under 20 equal and radial loads as shown in Fig. 8.14 These loads cause bending moment (M), tension or tangential force (T) and shear or radial force (V) as shown below [8-3]:

$$M = \frac{WR}{2}\left(\frac{\cos\chi}{\sin\theta} - \frac{1}{\theta}\right)$$

$$T = \frac{W\cos\chi}{2\sin\theta}$$

$$V = -\frac{W\sin\chi}{2\sin\theta}$$

The resulting values are listed in Table 8.3. The moment changes sign as a function of c. This is due to the fact that the ring is being forced from a circle into a 20-sided shape. The tension is the force between sectors and is constant. This results in a tensile stress on all cross sections. The shear force is highest at the pin holes.

Table 8.3
Loads on central ring.

Location	c (degree)	M (N-m)	T (N)	V (N)
Between pin holes	0,18,36,…	13830	3.2×10^6	0
At pin holes	9,27,45,…	-27620	3.2×10^6	0.5×10^6

Since the ring radius is large with respect to its section, one can use formulas for a straight beam to calculate stresses. The resulting error in this assumption is about ± 10% for either the extreme fibres on the inside radius or the outside radius [8-4]. The highest stresses will be near the edge of the hole due to stress concentration. The combined bending and tensile stresses can be calculated from:

$$\sigma = \frac{T}{A} + \frac{My}{I},$$

where:
A = Net cross sectional area,
I = area moment of inertia,
y = distance from the neutral axis.

This results in a tensile stress of 152 MPa at the edge of the hole, a tensile stress of 163 MPa at the ring outside radius at the hole location and a tensile stress of 97 MPa at the ring inside radius between the hole locations.

The stress concentration factor for edge of the hole is about 2.4 [8-5] and therefore, this location is most critical for cyclic loading. The stress at this location varies between 0 and 152 MPa as the magnet is cycled because of lack of preload.

Ring material is alloy steel AISI 4340 with properties as shown in Table 8.4. The notch sensitivity factor for this material and average machined surface is about 0.9. This gives a fatigue stress concentration factor of 2.2 for near the hole. The equivalent static stress for these conditions is 772 MPa. This gives a safety factor of 1.3 for infinite life. It must be noted that infinite life is defined as more than 10^6 cycles. Therefore a safety factor of 1.3 for infinite life is appropriate as the magnet is cycled very infrequently. From a strictly static point of view, the safety factor is about 6 to yielding for the highest stress location.

Table 8.4
Material properties for centre ring.

Yield strength	1000 MPa.
Tensile strength	1140 MPa
Hardness	34 RC
Elongation	15 %
Endurance limit	570 MPa (infinite life)
Working endurance	240 MPa (machined surface, 99% reliability, 0.7 size factor)

8.2.11 Pin Stress Analysis

The pin has a bending load of 1.0 MN. Assuming all of the load is applied at the end of the pin, i.e. worst load distributions, bending moment is 120000 N-m and maximum bending stress is 707 MPa on the surface. Therefore the stress varies between 0 and 707 MPa as the magnet is cycled because of lack of preload.

Pin material is alloy steel AISI 4340 with surface properties as shown in Table 8.5.

Table 8.5
Material properties on surface of pin.

Yield strength	1570 MPa.
Tensile strength	1950 MPa
Hardness	55 RC
Elongation	10 %
Endurance limit	975 MPa (infinite life)
Working endurance	464 MPa (ground surface, 99% reliability, 0.7 size factor)

No stress risers exist on the surface. The equivalent static stress for these conditions is 1550 MPa. This gives a safety factor of about 1 for infinite life. As in the ring this is justified due to the very low cycle rate. From a static point of view, the factor of safety is 2.2 to yielding.

The pin has a shear load of 1.0 MN, which gives a maximum shear stress of 118 MPa at the centre of the pin. Therefore, the principal stresses are 118 MPa and -118 MPa at the centre.

Properties of pin material at its centre are as shown in Table 8.6. No stress risers exist at the centre. The equivalent combined static stress for these conditions is 219 MPa. This gives a safety factor of 6 for infinite life.

Table 8.6
Material properties at centre of pin.

Yield strength	1350 MPa.
Tensile strength	1500 MPa
Hardness	45 RC
Elongation	12 %
Endurance limit	750 MPa (infinite life)
Working endurance	420 MPa (99% reliability, 0.7 size factor)

8.2.12 Sector Connection

Figure 8.16 shows a typical joint between the sectors. The joint is made via 2 pins and a plate. This joint is designed to be used on the tension side of the disk. The pins transfer the tensile load in shear to the plate. The plate is then loaded in tension.

It is important that a very good fit is achieved between the plate, the sectors and the pins. For this purpose it is anticipated that the pins and the plate would be machined to final dimensions. The sectors will also be fully machined, except for the size of the pin holes. They will be machined under size at the factory and be machined to final tolerances at site with the disk fully assembled. However, if the blocks are machined to a very high level of accuracy, it may be possible to preassemble all pinned connections at the factory for verification, then disassemble and ship to site and reassemble. The required level of accuracy has not yet been determined. We will discuss this with potential vendors.

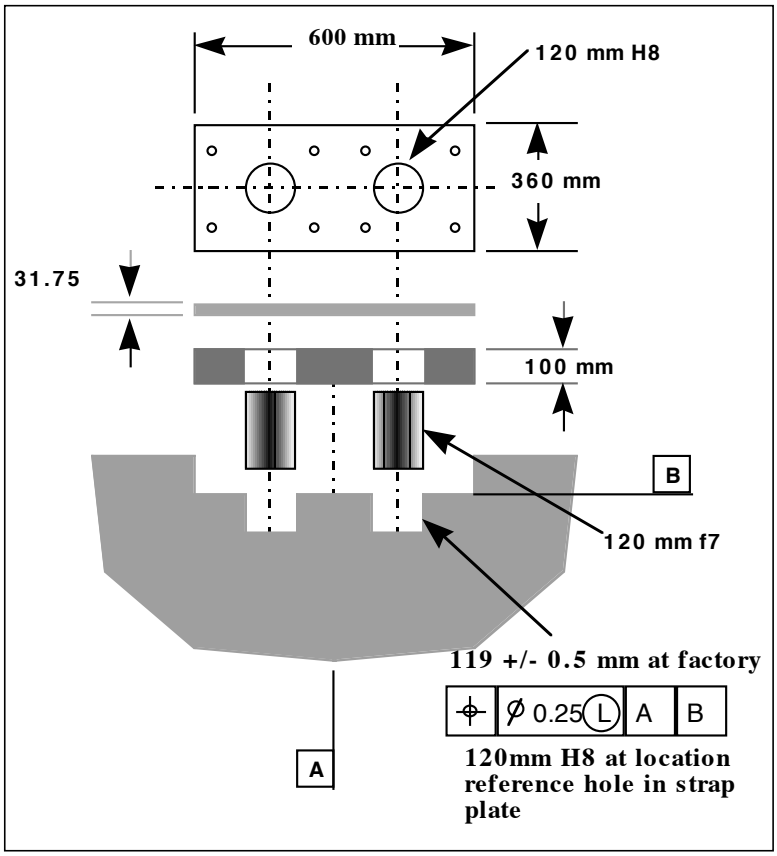

Fig. 8.16: Connection between sectors.

A cover plate is shown in the drawing. The plate serves two purposes:

1. To contain the pins against the magnetic force.
2. To provide a flat surface for mounting of other components, such as support posts for the chambers.

Cyclic loading analysis of the sector connections is similar to that for the centre ring and is being carried out in conjunction with studies of joint preload.

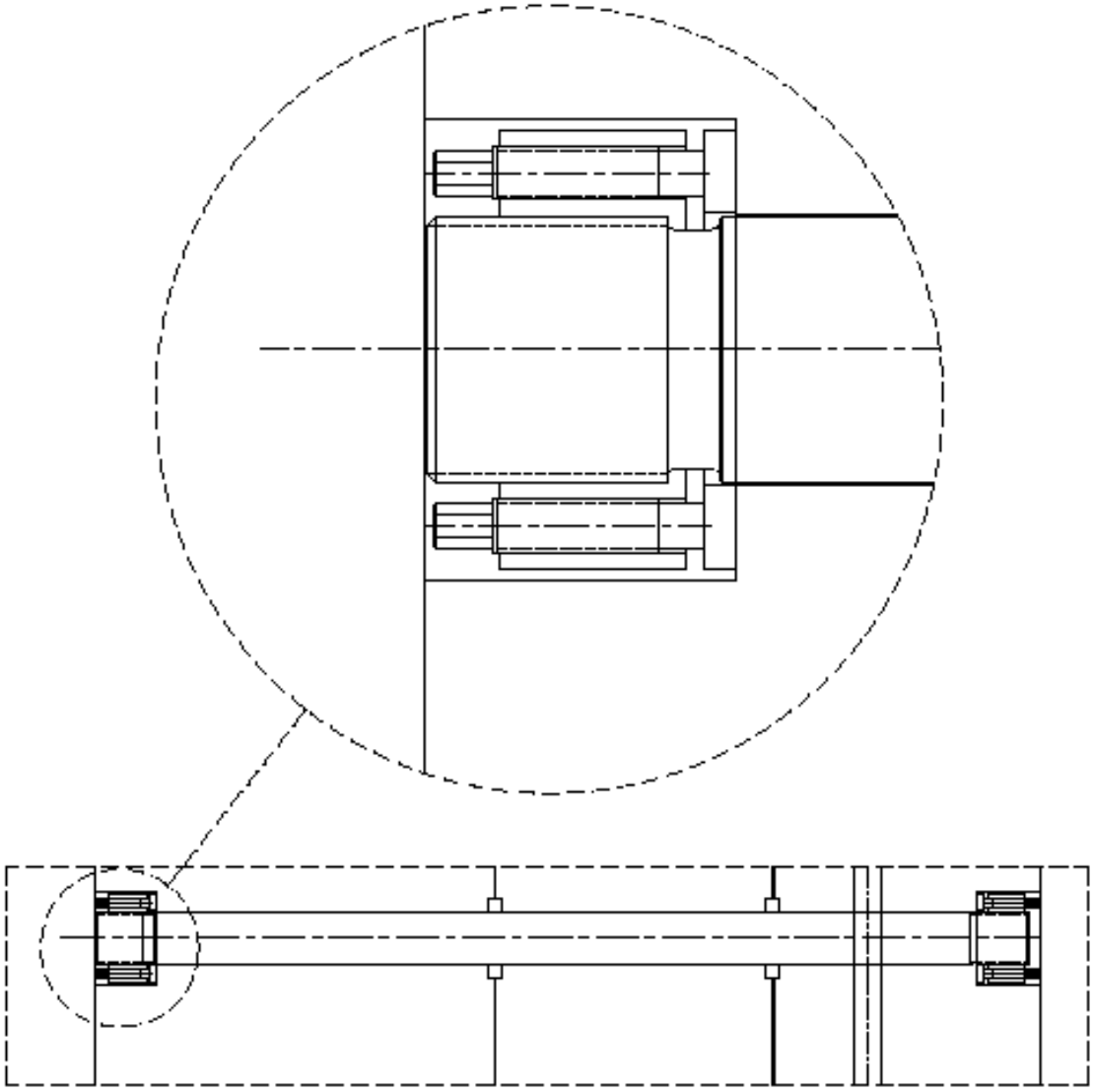

Fig. 8.17: Tie rod between nose and YE1 showing detail of nut.

8.2.13 Tie Rods

The maximum forces on the tie rods between the nose and YE1 is 2.62 MN for a 24-sector construction (section 0) For a 20-sector construction the maximum force would be about 3.1 MN. This gives a stress of 617 MPa for an 80 mm diameter tie rod.

The tie rod is made from alloy steel, AISI 4340 (EURONORM 83 35CrNiMo6), with

material properties as shown in Table 8.7.

Table 8.7
Material properties of tie rods.

Yield strength	980 MPa.
Tensile strength	1090 MPa
Hardness	38 RC
Elongation	12 %
Endurance strength	620 MPa (for 10^4 cycles)
Working strength	350 MPa (machined surface, 99% reliability, 0.7 size factor)

With this material the safety factor for static stress is 1.6. The effects of cycling loading and preload are under investigation at this time.

8.2.14 Disk Material

The material for the endcap will be low-carbon steel. This is the material of choice for its magnetic properties, however it has relatively low strength. The CMS endcap is under severe loading. This is in contrast to many conventional magnet yokes. A balance between good magnetic properties and moderate strength has to be achieved.

Chemical Requirements

The disk material will be AISI-SAE 1008 grade low carbon steel with chemical composition as shown in Table 8.8. Testing of each heat will be required to ensure compliance with these values.

Table 8.8
Disk material chemical composition.

Carbon	0.08% nominal, (0.10% max.)
Manganese	0.30% - 0.50%
Sulfur	0.05% max.
Phosphorous	0.04% max.

Mechanical Requirements

The mechanical properties of the disk steel material will be as shown in Table 8.9. These are nominal minimum values based on steel specifications.

Table 8.9
Disk material mechanical properties.

Yield Strength	240 MPa min
Tensile strength	350 MPa min
% elongation in 50 mm	22% min

As the rolled or forged plates for the endcap steel are very thick, it is anticipated that

mechanical properties will vary trough the thickness as well as with direction. Testing of the material will be required to ensure compliance with these minimum values at all locations within the plates and in directions normal and parallel to the surface.

Magnetic Requirements

The relative permeability of the steel material will be as shown in Table 8.10. As shown in the magnetic section, most of the endcap steel is in saturation. The induction is via the superconducting coil. Therefore the absolute value of relative permeability is not of primary concern. However, uniformity of permeability is very important as it has an impact on coil forces. Requirements for uniformity are under investigation at this time. It is anticipated that sectors cut from a single rectangular plate will be used on diametrically opposite sides of a disk to help ensure magnetic symmetry.

Table 8.10
Disk material magnetic properties.

Relative permeability at 1.8 Tesla	155 min
Variability among all pieces at 1.8 Tesla	155-165

Size and Tolerance

The size of the raw plate material and the tolerances on size and form are dependent on fabrication processes chosen by the vendor. The design shows finished blocks. It will be up to the vendor to procure material consistent with the finished block sizes.

8.2.15 Fabrication

The fabrication process is very dependent on the chosen design and the capabilities of the vendors. It is anticipated that the fabrication process should be generally as outlined below:

- Special thick plates of appropriate composition and size are manufactured at a steel mill. It should be noted that there are only a few places in the world that can make plates this thick. Once the thickness criterion is met, the overall size of the plate is of major concern. It is unlikely that many mills could produce a plate large enough to yield two sectors of a 20 sector construction. If only one sector is cut from a plate, the waste would be too great and most likely render the process uneconomical. In such a case a larger number of sectors would have to be chosen.
- Rolling of plates. It is anticipated that a moderate amount of rolling is required in the plates to achieve the proper mechanical strength. It is unlikely that many mills can produce plates thick enough to get the required amount of reduction. It is also unlikely that any other process, with the possible exception of forging, can render a useful plate. This, again, limits the number of mills that can produce these plates.
- Preassembly and/or welding of sectors. It is possible to weld, or equivalently fasten, smaller sections to form a sector. This can be chosen by steel mills who cannot make large enough plates.
- Cutting of plates. Plates are cut to form rough sectors. It is anticipated that only the sides of the block need to be cut and that the two faces of the block are left in the as rolled condition. The type and amount of cutting should be minimised. It should also be done to reduce the total amount of waste. Cutting as close to the net shape is,

of course, desirable as it minimises the machining.

- Weld repair. It may be necessary to repair damaged plates during the fabrication process. The damage may occur during cutting or may be due to a void in the plate, or other similar anomaly. This is allowed. The type of weld has not been determined. It is anticipated that most conventional welding processes will be acceptable.
- Block machining. Each block will have to be machined flat and true to form on three surfaces. The two surfaces mating with adjacent blocks and the surface mating to the centre ring. It is anticipated that the surfaces forming the outside of the disk are left as rough cut. However, holes and other features for mounting of muon chambers will be required on these surfaces. The last block is machined after assembly of remaining blocks.
- Machining of holes and other features. Locating features and hole are machined in pairs of blocks. This is done to ensure proper fit during assembly.
- Preassembly. Each disk is entirely assembled at the factory. This is a requirement. It is important that all mating surfaces and features be verified and corrections be made at the factory. If there are joints that can be assembled only once, it is important that they be verified and partial trial joint assemblies be made at this time. As mentioned earlier, this is not possible for a fully welded option. In this case, sufficient preassembly must be done to verify correct assembly on site.

8.2.16 Assembly

In figure 8.18 through figure 8.21, the assembly operations are schematically shown. The main point about this scheme is that it is erected vertically. This will save floor space and eliminates the need for a turning fixture. It can also be erected directly on the cart.

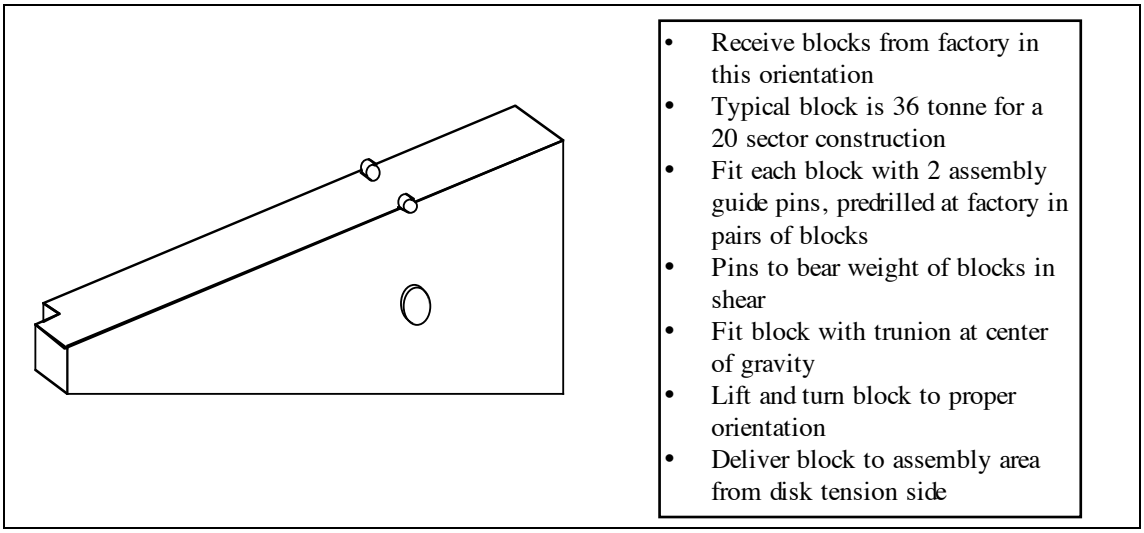

Fig. 8.18: Block pre-assembly preparation.

Horizontal assembly is also possible. This may have advantages in joint design and construction. However, it requires a very large turning fixture to make it vertical and other operations to position it on the cart. The vertical assembly is a goal to minimise time and space requirements.

8.2.17 Endcap Calorimeter Connection

The endcap calorimeter is attached to YE1 as one piece. The attachment scheme is shown in Fig. 8.22. The calorimeter is built in the horizontal position on the plate YN1. It is then turned o the vertical position as shown in this figure. The attachment is carried out by moving YE1 into position and engaging he conical interface. The main tie rods and on the outer radius and the smaller tie rods on the inner radius are then used to fasten the calorimeter in place. Fig. 8.23 shows the complete assembly.

Prior to calorimeter assembly, plate YN1 is fastened to YE1 and the magnetic test is conducted. This is done in order to have a complete magnetic assembly in place for the magnet test.

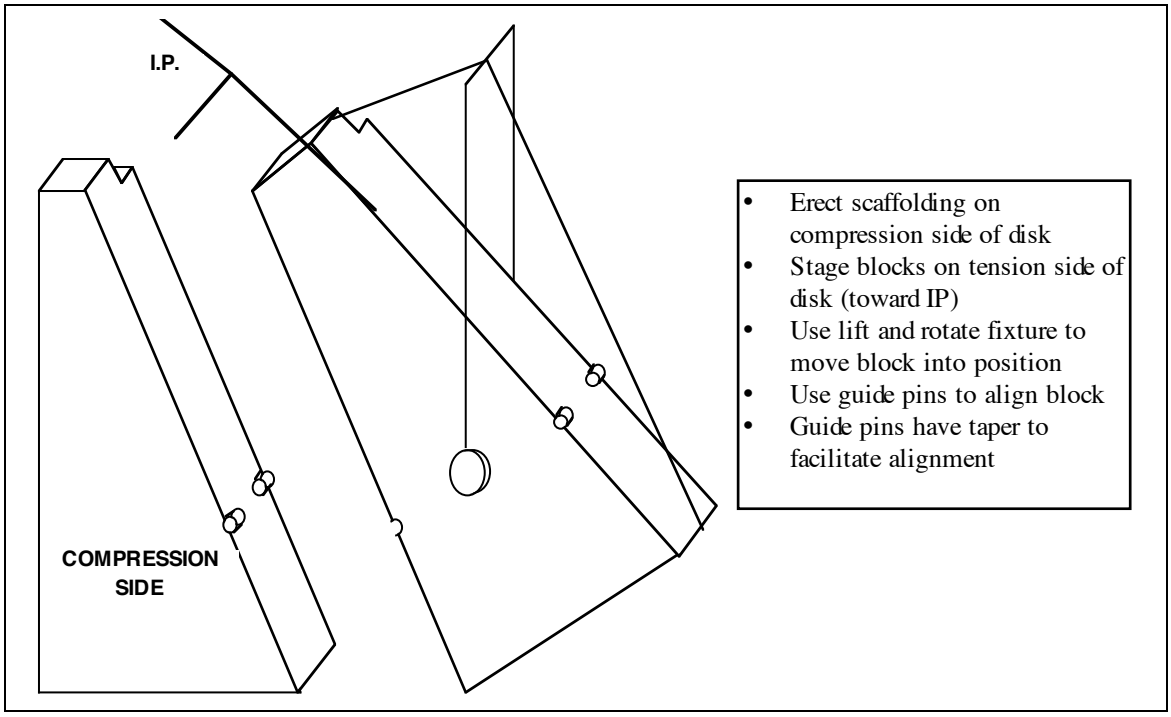

Fig. 8.19: Block rigging and positioning.

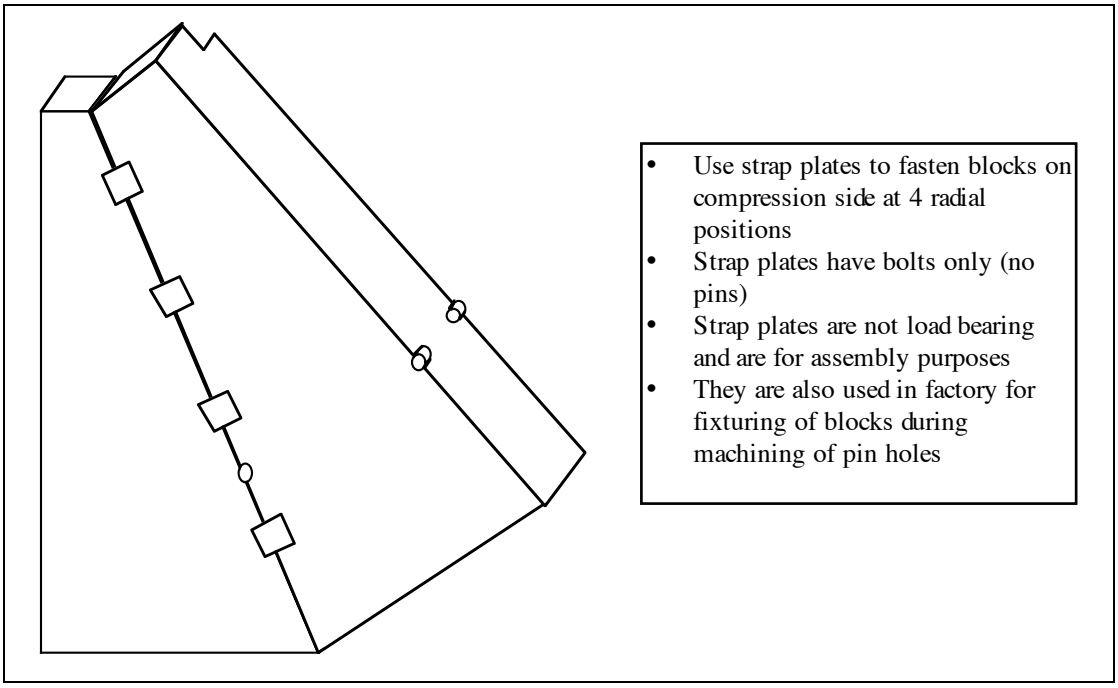

Fig. 8.20: Assembly of compression side (away from IP).

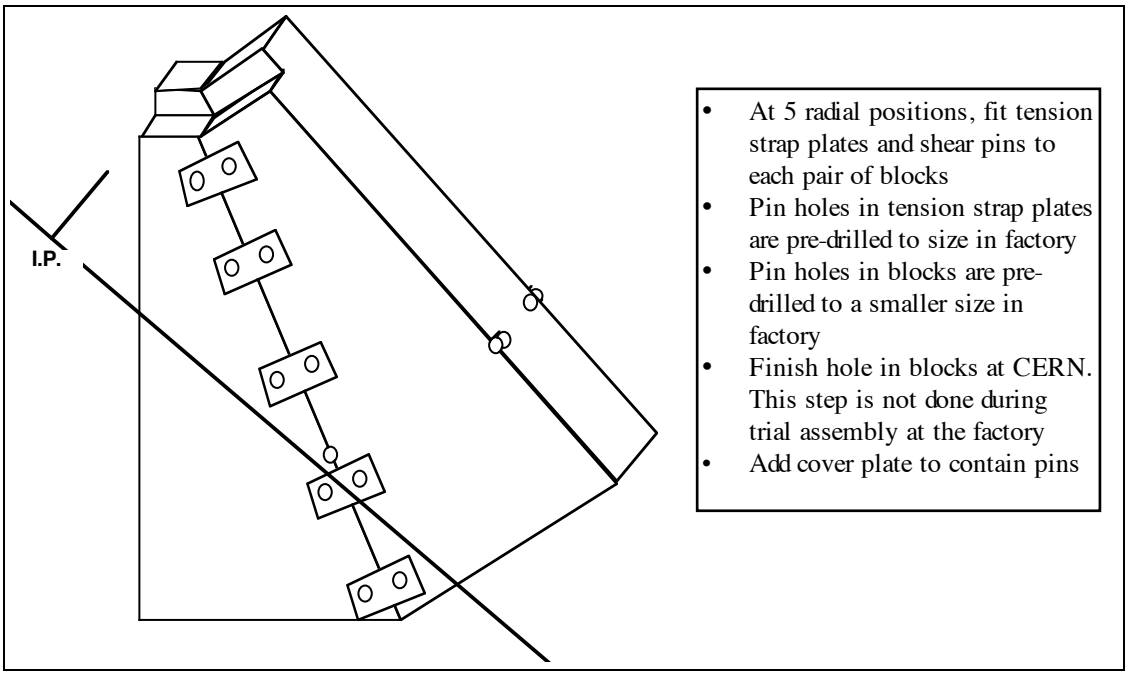

Fig. 8.21: Assembly of tension side (toward IP).

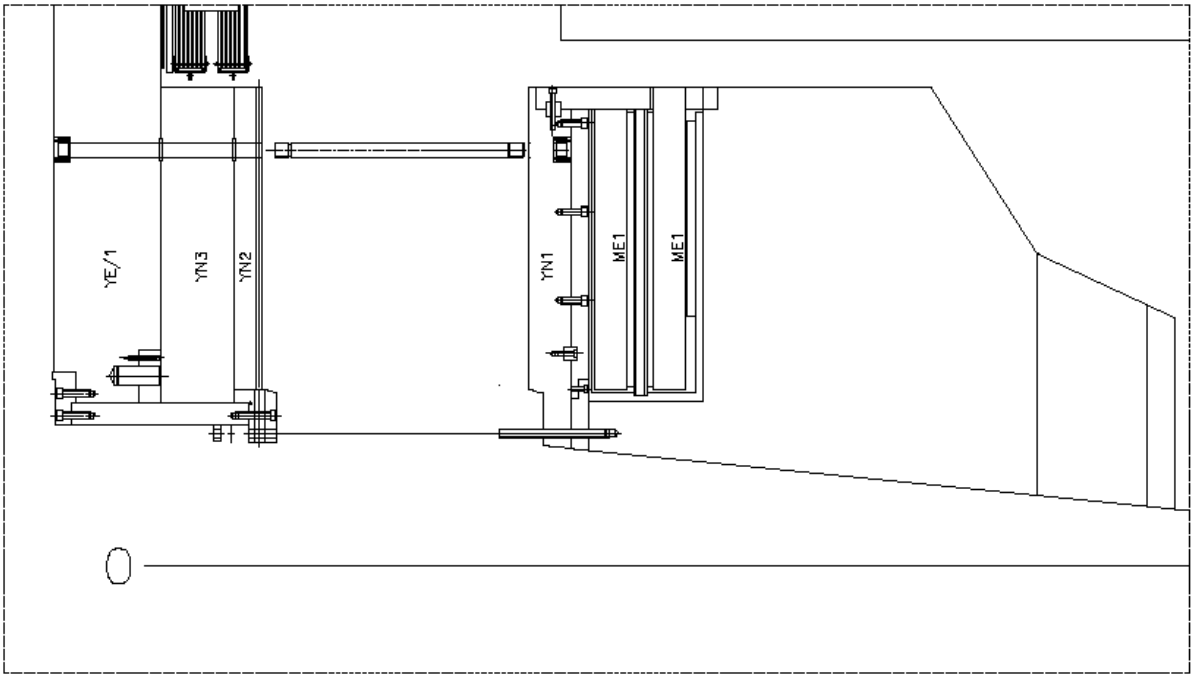

Fig. 8.22: Endcap calorimeter before attachment to YE1.

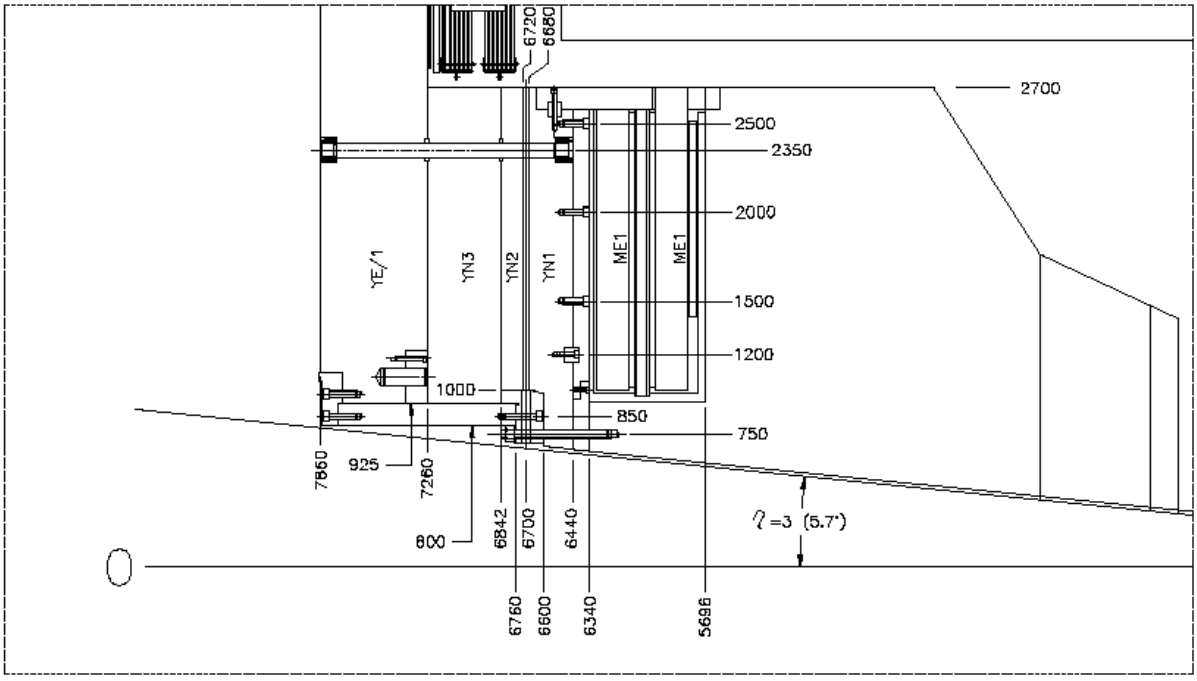

Fig. 8.23: Endcap calorimeter after attachment to YE1.

8.3 SUPPORT SYSTEM

This section contains the description of CMS endcap support and systems. There will be two endcaps. Each endcap consists of disks and each disk will have a separate cart. Therefore, there will be a total of 6 carts. The general arrangement of the carts is shown in Fig. 8.24. YE1 and the endcap calorimeter are shown in Fig. 8.25.

The carts will support the disks as they are installed in their final position within the CMS detector. They will also be used for support of the disks during construction on the surface hall, for motion of the disks during construction, and for detector opening and access.

Once all of the disks are fully constructed and instrumented with all detectors, the disks will be attached to form 2 integral endcaps. After this step, each endcap is one object and moves as one unit. The system is designed to use rollers, but studies going on to incorporate the same kind of air pad system that will be used for the barrel.

8.3.1 Stability

The disks are very large and relatively thin. A criterion for the stability must be chosen. We have designed for a width of support to height of centre of gravity ratio of 30%. This means that a force equal to 15% of disk weight is required to destabilise it. This is admittedly a large force, but the magnetic load on YE1 is about 7 times its weight. Obviously if the magnet is turned on while the disks are locked in any position but not closed fully against the barrel, the 15% lateral stability is insufficient and interlocks must be incorporated to avoid this situation.

The other issue is stability during possible earthquakes. At this writing, this has not been determined. We believe that the above criterion will satisfy this requirement.

Due to proximity of the disks, if all three disks were supported on one rail system, this number would be only 14%, which is quite low. Once we decide to support on two rails, 30% is easily attainable by alternating the support points between the inner and outer rails.

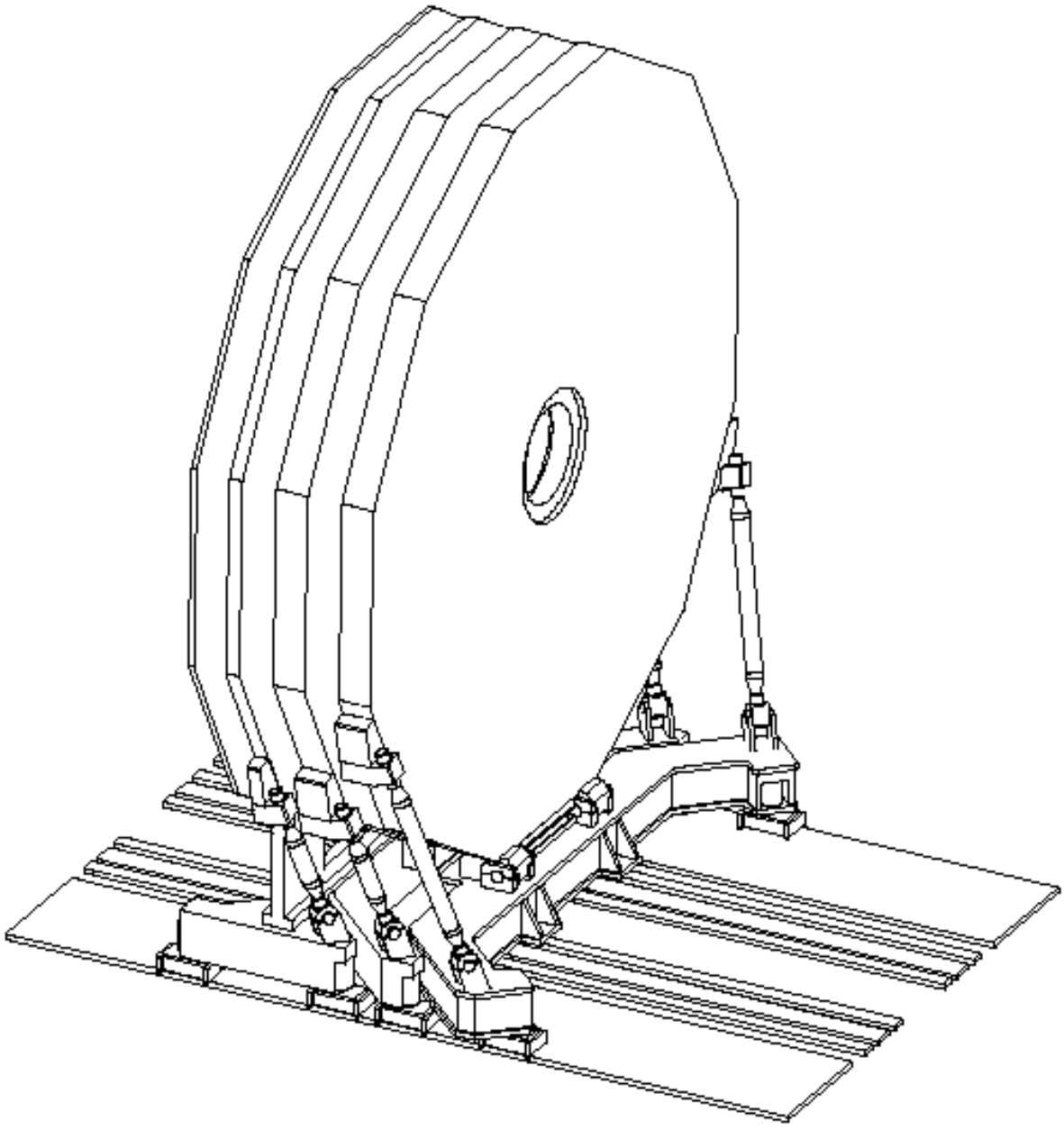

Fig. 8.24: Endcap disks shown on their individual carts in the closed position (ME4 shield wall is also shown).

8.3.2 Cart Design

Below are design parameters for each of the carts. YE1 cart had the most demanding requirements because of the large cantilever load of the endcap calorimeter.

- Each cart has a set of four movers which consist either of a roller or airpad with a hydraulic cylinder directly on top. The choice between rollers and airpads is currently under investigation.
- The movers are on inner and outer set of rails alternatively for YE1 and YE2, and on the outer rails for YE3.
- Each cart has a pair of braces to stabilise the disks. The braces reach as high on the

disk as possible. This is particularly important for YE1 where the brace reaches to 4 and 8 o'clock positions.

- Each brace had provisions for length adjustment to position the disk vertically.
- Each cart has a hinge connection to the disk. This is required due to the distortion in the disk as a result of the magnetic force.
- Each disk has an extension into the cart between the hinge shafts. This is designed such that if the braces were removed the disk will not fall.
- Each cart has provisions to rest on the inboard set of rails on sliding plates directly under the centre of gravity.

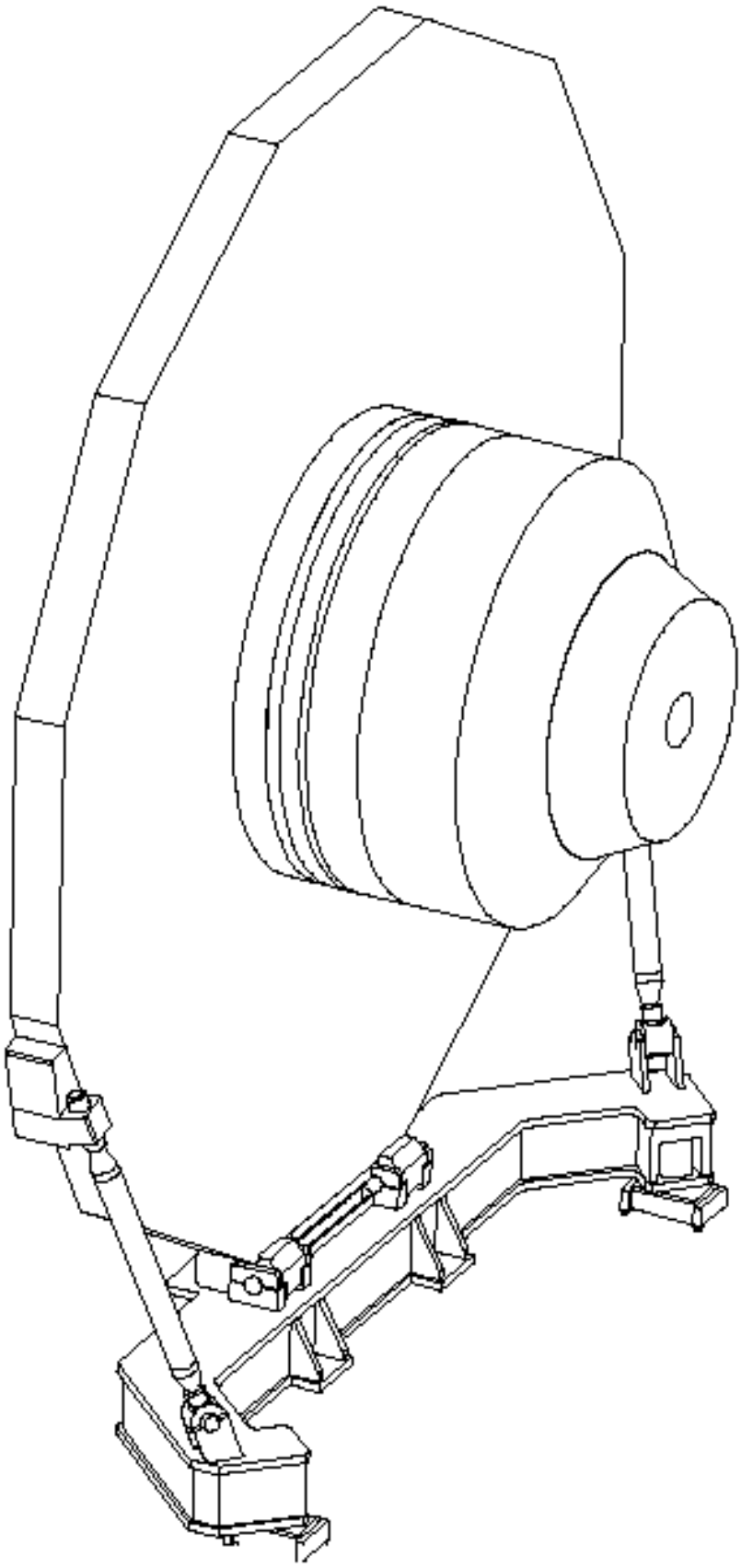

Fig. 8.25: YE1 disk on its cart with endcap calorimeter attached.

8.3.3 Operation

- Below is a general description of the operation of the support system.
- The endcap rides on the movers with the main jacks locked at a height slightly above final height.
- The endcap is brought close to the barrel but not touching.
- The main jacks are unlocked and the disks are lowered, with height control, on all four jacks to keep them level.
- The disks are set on grease pads which are on the inboard rails and under the centre of gravity. This sets the vertical position at the final height.
- Connections to barrel are engaged. These will be 4 hydraulic cylinders at f angle of roughly 75, 115, 255, 285 and accessible from the walkways.
- The main jacks are unloaded to a nominal constant force (pressure) of about 50 tonnes each. This maintains contact between rollers and the rails.
- The endcap is pulled on the grease pad against the barrel by the hydraulic cylinders.
- The hydraulic cylinders are maintained at a constant force. This force is greater than what is required to keep the disk from going downhill.
- The magnet is energised.
- The grease pads and the rollers allow the perimeter of the disk to move in Z away from the IP. Most of the load is on the grease pads.
- By maintaining only a small pressure in the main jacks, the cart and the brace will not be overstressed. The hinge between the disk and cart also aids in this respect.
- The hydraulic cylinders also allow this motion but maintain a constant force against the barrel.
- This procedure requires the operation of the main jacks in two modes: position control and force control. The hydraulic supply units must be capable of both modes. The hydraulic systems must be active during detector operation and appropriate interlocks must be incorporated.